

BAYESIAN VARIATIONAL APPROXIMATION FOR THE JOINT DETECTION ESTIMATION OF BRAIN ACTIVITY IN fMRI

Lotfi Chaari¹, Florence Forbes¹, Philippe Ciuciu², Thomas Vincent² and Michel Dojat³

¹ INRIA Rhône-Alpes
655 avenue de l'Europe, Montbonnot
38334 Saint Ismier Cedex, France
firstname.lastname@inrialpes.fr

² CEA/DSV/I²BM/Neurospin, CEA
Saclay, Bbt. 145, Point Courrier 156,
91191 Gif-sur-Yvette cedex, France
firstname.lastname@cea.fr

³ Grenoble Institut des Neurosciences
BP 170 - F38042 Grenoble Cedex 09
France
Michel.Dojat@ujf-grenoble.fr

ABSTRACT

We address the issue of jointly detect brain activity and estimate brain hemodynamics from functional MRI data. To this end, we adopt the so-called JDE framework introduced in [1] and augmented in [2] with hidden Markov field models to account for spatial dependencies between voxels. This latter spatial addition is essential but also responsible for high computation costs. To face the intractability induced by Markov models, inference in [2] is based on intensive simulation methods (MCMC). In this work we propose an alternative to face this limitation by recasting the JDE framework into a missing data framework and to derive an EM algorithm for inference. We address the intractability issue by considering variational approximations. We show that the derived Variational EM algorithm outperforms the MCMC procedure on realistic artificial fMRI data.

Index Terms— Variational EM, MRF, Biomedical signal detection, Magnetic resonance imaging.

1. INTRODUCTION

Functional Magnetic Resonance Imaging (fMRI) is a powerful tool to non-invasively study the relation between cognitive task and cerebral activity through the analysis of the hemodynamic BOLD signal [3]. Within-subject analysis in event-related fMRI first relies on (i) a detection step to localize which parts of the brain are activated by a given stimulus type, and second on (ii) an estimation step to recover the temporal dynamics of the brain response. Most approaches to detect neural activity rely on a single *a priori* model for the temporal dynamics of activated voxels also known as the hemodynamic response function (HRF) [4]. A canonical HRF is usually assumed for the whole brain although there has been evidence that this response can vary with space or region, across subjects and groups [5]. In addition, a robust and accurate estimation of the HRF is possible only in regions that elicit an evoked response to an experimental stimulus [6]. Both issues of properly detecting evoked activity and estimating the HRF then play a central role in fMRI data analysis. They are usually dealt with independently with no possible feedback although both issues are strongly connected one to another. To introduce more flexibility regarding the assumptions on the HRF model, a novel approach referred to as the Joint Detection Estimation (JDE) framework has been introduced in [1] and extended in [2] to account for spatial correlation between neighboring voxels in the brain volume (regular lattice in 3D). In this latter approach, the HRF can be estimated while simultaneously detecting activity, in a region-based analysis, that is on a set of pre-specified regions of interest (ROI), also named *parcels*. This approach is mainly based on: (i) the non-parametric modelling of the HRF at a regional spatial scale (parcel-level) that provides a fair compromise between homogeneity of the BOLD signal and reproducibility of the HRF estimate; (ii) prior information about the temporal smoothness of the HRF to

be estimated; and (iii) the modelling of spatial correlation between neighboring voxels within each parcel using condition-specific hidden Markov fields. In [1, 2], posterior inference is carried out in a Bayesian setting using Monte Carlo Markov Chain (MCMC) methods, which requires in the spatial case, Swendsen-Wang or partial decoupling algorithms to guarantee rapid convergence given the spatial dependencies.

In this paper, we reformulate the approach derived in [2] into a missing data framework and propose a simplification of the inference framework. As a more computationally efficient alternative to MCMC, we resort to variational approximation techniques using a Variational Expectation Maximization algorithm (VEM) in order to derive estimates of the HRF, the Neural Response Levels (NRLs) and the corresponding labels (activating/non-activating voxels). Preliminary experiments on realistic artificial data sets are reported to demonstrate the good performance of our approach both in terms of computation time and estimation quality. The results compare favorably: for a given fixed amount of computational resources, the variational approach outperforms the MCMC one. This potentially increases considerably the impact of the JDE framework making its application possible in larger range brain MRI studies.

2. A JOINT DETECTION-ESTIMATION MODEL

Capital letters indicate random variables, and lower case their realizations. Matrices are denoted with bold upper case letters (eg \mathbf{P}). A vector is by convention a column vector. The transpose is denoted by t . Unless stated otherwise, subscripts i , m , k and n are respectively indexes over voxels, stimulus types, mixture components and time point. The Gaussian distribution with mean $\boldsymbol{\mu}$ and variance $\boldsymbol{\Sigma}$ is denoted using $\mathcal{N}(\boldsymbol{\mu}, \boldsymbol{\Sigma})$.

2.1. Missing and observed variables

We first recast the parcel-based model of the BOLD signal described in [2] in a missing data framework. For a given parcel V , the observed data is denoted by $Y = \{Y_i, i \in V\}$ where Y_i is a N -dimensional vector representing the fMRI time course measured in voxel $i \in V$ at times $(t_n)_{n=1:N}$, where $t_n = nTR$, N being the number of scans and TR , the time of repetition. Additional non observed variables are introduced: 1) The neural response levels $A = \{A_m, m = 1 : M\}$ with $A_m = \{A_{mi}, i \in V\}$ where M is the number of experimental conditions (or stimulus types). We will also use the notation $A_i = \{A_{mi}, m = 1 : M\}$; 2) The HRF function denoted by $H = [H_0, H_{\Delta t}, \dots, H_{D\Delta t}]^t$ is a $(D+1)$ -real valued vector; 3) The activation class assignments $Z = \{Z_m, m = 1 : M\}$ with $Z_m = \{Z_{mi}, i \in V\}$ represent the *activation classes* for each voxel, in each of the M experimental conditions. $Z_{mi} = k$ means that voxel i lies in activation class k for the m th experimental condition. Typically the number of classes is $K = 2$ for activating and non activating voxels. The observed and missing variables are

then linked through the following relationship implying additional parameters to be estimated or fixed as specified bellow. Each Y_i reads

$$\forall i \in V, \quad Y_i = \sum_{m=1}^M A_{mi} \mathbf{X}_m H + \mathbf{P} \ell_i + \varepsilon_i, \quad (1)$$

where $\mathbf{X}_m = (x_{t_n - d\Delta t}^m)_{n=1:N, d=0:D}$ denotes the $N \times (D+1)$ binary matrix that codes the arrival times of the m th stimulus which are approximated to fit a Δt -sampled grid, where Δt is the sampling period of the HRF ($\Delta t < TR$); ε_i 's stand for the noise and are independent and normally distributed, $\varepsilon_i \sim \mathcal{N}(\mathbf{0}, \Gamma_i^{-1})$, and \mathbf{P} is the low frequency orthogonal $N \times L$ matrix which accounts for physiological artifacts. It consists of an orthonormal basis of L functions $[P_1 | \dots | P_L]$. We denote by $\ell = \{\ell_i, i \in V\}$ the set of low frequency drifts. Each ℓ_i is a L -dimensional vector of regressors to be estimated. We denote by $\Gamma = \{\Gamma_i, i \in V\}$ the set of all precision matrices.

2.2. Hierarchical model of the complete data distribution

With standard additional assumptions, not detailed here, and omitting the dependence on the parameters to be specified later, the distribution of both the observed and missing variables can be decomposed as follows:

$$p(y, a, h, z) = p(y | a, h) p(a | z) p(h) p(z).$$

To fully define the model, we now specify each term in turn.

The $p(y | a, h)$ term. From (1), it comes that:

$$p(y | a, h) = \prod_{i \in V} p(y_i | a_i, h)$$

$$\text{with } Y_i | A_i = a_i, H = h \sim \mathcal{N} \left(\sum_{m=1}^M a_{mi} \mathbf{X}_m h + \mathbf{P} \ell_i, \Gamma_i^{-1} \right).$$

The $p(a | z)$ term. Regarding NRLs, it is standard to assume that different types of stimuli induce statistically independent NRLs. The allocation variables Z_{mi} are then introduced to segregate activating voxels from non-activating ones. Among voxels, the NRLs are assumed to be independent conditionally on Z_m so that putting together all experimental conditions we get:

$$p(a | z) = \prod_{m=1}^M \prod_{i \in V} p(a_{mi} | z_{mi}), \quad (2)$$

where we further assume that the right hand side is defined by $A_{mi} | Z_{mi} = k \sim \mathcal{N}(\mu_{mk}, \sigma_{mk}^2)$. The Gaussian parameters are unknown and denoted by $\boldsymbol{\mu}$ and $\boldsymbol{\sigma}$ with $\boldsymbol{\mu} = \{\boldsymbol{\mu}_m, m = 1 : M\}$ and $\boldsymbol{\mu}_m = [\mu_{m1} \dots \mu_{mK}]^t$ and $\boldsymbol{\sigma} = \{\boldsymbol{\sigma}_m, m = 1 : M\}$ with $\boldsymbol{\sigma}_m = [\sigma_{m1} \dots \sigma_{mK}]^t$.

The $p(h)$ term. Akin to [7, 8], we introduce constraints in the prior that favor smooth variations in h :

$$H \sim \mathcal{N}(\mathbf{0}, \sigma_h^2 \mathbf{R}) \quad \text{with} \quad \mathbf{R} = (\Delta t)^4 (\mathbf{D}_2^t \mathbf{D}_2)^{-1}$$

where \mathbf{D}_2 is the second-order finite difference matrix and σ_h^2 is a parameter to be estimated or fixed. Moreover, the extreme time points of the HRF are constrained to zero [8].

The $p(z)$ term. As in [2], we assume prior independence between experimental conditions regarding the activation class assignments. It follows that

$$p(z) = \prod_{m=1}^M p(z_m; \beta_m)$$

where we assumed in addition that $p(z_m; \beta_m)$ is a K-class Potts model with interaction parameter β_m ,

$$p(z_m; \beta_m) = W(\beta_m)^{-1} \exp(\beta_m \sum_{i \in V} \sum_{j \in \mathcal{N}(i)} \delta(z_{mi}, z_{mj})),$$

where $\delta(z_{mi}, z_{mj})$ is 1 when $z_{mi} = z_{mj}$ and 0 otherwise, $W(\beta_m)$ is the normalizing constant and $\mathcal{N}(i)$ denotes the voxels that are neighbors to voxel i on the 3D brain volume. The unknown parameters are then $\boldsymbol{\beta} = \{\beta_m, m = 1 : M\}$.

For the complete model, it follows that the whole set of parameters denoted by $\theta \in \Theta$ is $\theta = \{\Gamma, \ell, \boldsymbol{\mu}, \boldsymbol{\sigma}, \sigma_h, \boldsymbol{\beta}\}$. Note that H could also be considered as a parameter but it distinguishes from θ as priors are not necessarily available for the parameters in θ . If they were, they could be incorporated easily.

3. ESTIMATION BY VARIATIONAL EM

We propose to use an Expectation-Maximization (EM) framework [9] to deal with the missing data namely, $A \in \mathcal{A}$, $H \in \mathcal{H}$, $Z \in \mathcal{Z}$. Let \mathcal{D} be the set of all probability distributions on $\mathcal{A} \times \mathcal{H} \times \mathcal{Z}$. EM can be viewed [10] as an alternating maximization procedure of a function F such that for any $q \in \mathcal{D}$, $F(q, \theta) = \mathbb{E}_q[\log p(y, A, H, Z; \theta)] + I[q]$ where $I[q] = -\mathbb{E}_q[\log q(A, H, Z)]$ is the entropy of q , and $\mathbb{E}_q[\cdot]$ denotes the expectation with respect to q . Denoting current parameter values by $\theta^{(r)}$, the alternating procedure proceeds as follows:

$$\text{E-step: } q^{(r)} = \arg \max_{q \in \mathcal{D}} F(q, \theta^{(r)}) \quad (3)$$

$$\text{M-step: } \theta^{(r+1)} = \arg \max_{\theta \in \Theta} F(q^{(r)}, \theta) \quad (4)$$

However, the optimization step in Eq. (3) leads to $q^{(r)}(a, h, z) = p(a, h, z | y; \theta^{(r)})$, which is intractable for non trivial models. Hence, we propose to use an EM variant in which the E-step is instead solved over a restricted class of probability distributions, $\tilde{\mathcal{D}}$, chosen as the set of distributions that factorize as $q(a, h, z) = q_A(a) q_H(h) q_Z(z)$ where $q_A \in \mathcal{D}_A$, $q_H \in \mathcal{D}_H$ and $q_Z \in \mathcal{D}_Z$, the sets of probability distributions on \mathcal{A} , \mathcal{H} , \mathcal{Z} respectively.

The fact that the HRF H can be equivalently considered as missing variables or random parameters induces some similarity between our Variational EM variant and the Variational Bayesian EM algorithm presented in [11]. Our framework varies slightly from the case of conjugate exponential models described in [11] and more importantly, our presentation offers the possibility to deal with extra parameters (θ) for which no prior information is available. As a consequence, the variational Bayesian M-step of [11] is transferred into our E-step while our M-step has no equivalent in the formulation of [11]. It follows then that the E-step becomes an approximate E-step that can be further decomposed into three stages in which the goal is to update q_H , q_A and q_Z in turn using three equivalent expressions of F when q factorizes in $\tilde{\mathcal{D}}$. At iteration (r), with current estimates denoted by $q_A^{(r-1)}$, $q_Z^{(r-1)}$ and $\theta^{(r)}$, the updating rules become (using the Kullback-Leibler divergence properties):

$$\text{E-H: } q_H^{(r)}(h) \propto \exp \left(\mathbb{E}_{q_A^{(r-1)} q_Z^{(r-1)}} [\log p(h | y, A, Z; \theta^{(r)})] \right)$$

$$\text{E-A: } q_A^{(r)}(a) \propto \exp \left(\mathbb{E}_{q_H^{(r)} q_Z^{(r-1)}} [\log p(a | y, H, Z; \theta^{(r)})] \right)$$

$$\text{E-Z: } q_Z^{(r)}(z) \propto \exp \left(\mathbb{E}_{q_A^{(r)} q_H^{(r)}} [\log p(z | y, A, H; \theta^{(r)})] \right).$$

The corresponding **M-step** is (since θ and $I[q]$ are independent):

$$\text{M: } \theta^{(r+1)} = \arg \max_{\theta \in \Theta} \mathbb{E}_{q_A^{(r)} q_H^{(r)} q_Z^{(r)}} [\log p(y, A, H, Z; \theta)].$$

For the **E-H** and **E-A** steps it follows from standard algebra that $q_H^{(r)}$ and $q_A^{(r)}$ are both Gaussian distributions: $q_H^{(r)} \sim \mathcal{N}(\mathbf{m}_H^{(r)}, \Sigma_H^{(r)})$ and $q_A^{(r)} = \prod_{i \in V} q_{A_i}^{(r)}$ with $q_{A_i}^{(r)} \sim \mathcal{N}(\mathbf{m}_{A_i}^{(r)}, \Sigma_{A_i}^{(r)})$. More specifically,

assuming current values for the $\mathbf{m}_{A_i}^{(r-1)}$, $\Sigma_{A_i}^{(r-1)}$ and $q_{Z_{mi}}^{(r-1)}(k)$, the r^{th} iteration starts with:

• **E-H step:** compute $\Sigma_H^{(r)} = \bar{Q}^{(r-1)}$ and $\mathbf{m}_H^{(r)} = \Sigma_H^{(r)} \bar{y}^{(r)}$, with

$$\begin{aligned} \bar{y}^{(r)} &= \sum_{i \in V} \left(\sum_{m=1}^M \mathbf{m}_{A_i}^{(r-1)}(m) \mathbf{X}_m \right)^t \Gamma_i^{(r)} (y_i - \mathbf{P} \ell_i^{(r)}) \\ \bar{Q}^{(r)} &= \mathbf{R}^{-1} / \sigma_h^2 + \sum_{i \in V} \left(\sum_{m, m'} \Sigma_{A_i}^{(r-1)}(m, m') \mathbf{X}_m^t \Gamma_i^{(r)} \mathbf{X}_{m'} \right. \\ &\quad \left. + \left(\sum_{m=1}^M \mathbf{m}_{A_i}^{(r-1)}(m) \mathbf{X}_m \right)^t \Gamma_i^{(r)} \left(\sum_{m=1}^M \mathbf{m}_{A_i}^{(r-1)}(m) \mathbf{X}_m \right) \right). \end{aligned}$$

The notation $\mathbf{m}_{A_i}^{(r-1)}(m)$ and $\Sigma_{A_i}^{(r-1)}(m, m')$ above indicates the m , resp. (m, m') , component of the corresponding vector, resp. matrix.

• **E-A step:**

$$\begin{aligned} \Sigma_{A_i}^{(r)} &= \left(\sum_{k=1}^K \Delta_{ki}^{(r)} + \tilde{\mathbf{H}}_i^{(r)} \right)^{-1} \\ \text{and } \mathbf{m}_{A_i}^{(r)} &= \Sigma_{A_i}^{(r)} \left(\sum_{k=1}^K \Delta_{ki}^{(r)} \boldsymbol{\mu}_k^{(r)} + \tilde{\mathbf{X}}_i^{(r)t} \mathbf{m}_H^{(r)} \right) \end{aligned}$$

with $\boldsymbol{\mu}_k^{(r)} = [\mu_{1k} \dots \mu_{Mk}]^t$ and for every $i \in V$, $\Delta_{ki}^{(r)} = \text{diag}_M [q_{Z_{1i}}^{(r-1)}(k)/\sigma_{1k}^{2(r)}, \dots, q_{Z_{Mi}}^{(r-1)}(k)/\sigma_{Mk}^{2(r)}]$, $\tilde{\mathbf{H}}_i^{(r)}$ is defined via its (m, m') components given by

$$\tilde{\mathbf{H}}_{i(m, m')}^{(r)} = \text{tr}(\Sigma_H^{(r)} \mathbf{X}_m^t \Gamma_i^{(r)} \mathbf{X}_{m'}) + \mathbf{m}_H^{(r)t} \mathbf{X}_m^t \Gamma_i^{(r)} \mathbf{X}_{m'} \mathbf{m}_H^{(r)}$$

and $\tilde{\mathbf{X}}_i^{(r)} = [g_1^t | \dots | g_M^t]^t$ with $g_m = \Gamma_i^{(r)} (y_i - \mathbf{P} \ell_i^{(r)})^t \mathbf{X}_m$. For the **E-Z** step, it comes

$$q_Z^{(r)}(z) = \prod_{m=1}^M q_{Z_m}^{(r)}(z_m) \quad (5)$$

$$\text{with } q_{Z_m}^{(r)}(z_m) = p_m(z_m | A_m = \mathbf{m}_A^{(r)}(m); \boldsymbol{\sigma}_m^{(r)}, \beta_m^{(r)})$$

where p_m is a Potts model with interaction parameter $\beta_m^{(r)}$ and external field $\boldsymbol{\alpha}_m^{(r)} = \{\boldsymbol{\alpha}_{mi}^{(r)}, i \in V\}$

with $\boldsymbol{\alpha}_{mi}^{(r)} = \Sigma_{A_i}^{(r)}(m, m) [1/\sigma_{m1}^{2(r)} \dots 1/\sigma_{mK}^{2(r)}]^t$ i.e.

$$\begin{aligned} p_m(z_m; \boldsymbol{\sigma}_m^{(r)}, \beta_m^{(r)}) &\propto \exp \left\{ \sum_{i \in V} \left(\boldsymbol{\alpha}_{mi}^{(r)}(z_{mi}) + \right. \right. \\ &\quad \left. \left. \beta_m^{(r)} \sum_{j \in \mathcal{N}(i)} \delta(z_{mi}, z_{mj}) \right) \right\}. \end{aligned}$$

The expression in (5) is intractable but a number of approximation techniques are available. In particular, we can use a mean-field like algorithm (fixing the neighbours to their mean value) as described in [12] in which $q_{Z_m}(z_m)$ can be approximated by $\tilde{q}_{Z_m}(z_m) = \prod_{i \in V} \tilde{q}_{Z_{mi}}(z_{mi})$ with, if $z_{mi} = k$, $\tilde{q}_{Z_{mi}}(k) \propto \mathcal{N}(\mathbf{m}_{A_i}(m); \mu_{mk}, \sigma_{mk}^2) p_m(Z_{mi} = k | \tilde{z}_{m\mathcal{N}(i)}; \beta_m, \boldsymbol{\sigma}_m)$, where \tilde{z}_m is a particular configuration of Z_m updated at each iteration according to a specific scheme and $p_m(z_{mi} | \tilde{z}_{m\mathcal{N}(i)}; \beta_m, \boldsymbol{\sigma}_m) \propto \exp\{\boldsymbol{\alpha}_{mi}(z_{mi}) + \beta_m \sum_{j \in \mathcal{N}(i)} \delta(\tilde{z}_{jm}, z_{mi})\}$ and $\tilde{z}_{m\mathcal{N}(i)} = \{\tilde{z}_{mj}, j \in \mathcal{N}(i)\}$.

$\mathcal{N}(i)\}$. See [12] for details. The **M-step** can also be divided into four sub-steps involving separately $(\boldsymbol{\mu}, \boldsymbol{\sigma})$, σ_h , β and (ℓ, Γ) :

• **M- $(\boldsymbol{\mu}, \boldsymbol{\sigma})$ step.** Updating parameters $\boldsymbol{\mu}$ and $\boldsymbol{\sigma}$ is straightforward as closed-form expressions are available:

$$\begin{aligned} \mu_{mk}^{(r+1)} &= \frac{\sum_{i \in V} q_{Z_{mi}}^{(r)}(k) \mathbf{m}_{A_i}^{(r)}(m)}{\sum_{i \in V} q_{Z_{mi}}^{(r)}(k)} \quad \text{and} \\ \sigma_{mk}^{2(r+1)} &= \frac{\sum_{i \in V} q_{Z_{mi}}^{(r)}(k) \left((\mathbf{m}_{A_i}^{(r)}(m) - \mu_{mk}^{(r+1)})^2 + \Sigma_{A_i}^{(r)}(m, m) \right)}{\sum_{i \in V} q_{Z_{mi}}^{(r)}(k)} \end{aligned}$$

• **M- σ_h^2 step.** This step is also closed-form:

$$\sigma_h^{2(r+1)} = \frac{\text{trace} \left((\Sigma_H + \mathbf{m}_H \mathbf{m}_H^t) \mathbf{R}^{-1} \right)}{D - 1}.$$

The other two M-steps are not closed-form and involved some numerical procedures. For β , the update can be solved using a mean field like approximation as done in [12]. For (ℓ, Γ) it is easy to show that they satisfy some fixed point equation not detailed here and to be solved numerically.

4. ILLUSTRATIONS

4.1. Simulated fMRI data

We simulated a random mixed sequence of indexes coding for $M = 2$ different stimuli. These two sets of trials (30 trials per stimulus) were then multiplied by stimulus-dependent and space-varying NRLs, which were generated according to the distribution in Eq. (2) (cf Fig. 1 left column). To this end, we generated 2D slices (cf Fig. 2 left column) composed of 20 x 20 binary labels Z_m (activating and non-activating voxels) for each stimulus type m . Then, we simulated normally-distributed NRLs:

$$\begin{aligned} A_{1i} | Z_{1i} = 0 &\sim \mathcal{N}(0, 0.3), & A_{1i} | Z_{1i} = 1 &\sim \mathcal{N}(2, 0.3), \\ A_{2i} | Z_{2i} = 0 &\sim \mathcal{N}(0, 0.5), & A_{2i} | Z_{2i} = 1 &\sim \mathcal{N}(2.8, 0.5). \end{aligned}$$

Fig. 1 illustrates the impact of the spatial correlation on the NRL maps. As illustrated in Fig. 3, the simulated fMRI data at each voxel i is obtained by adding a white Gaussian noise ε_i and low-frequency drift $\mathbf{P} \ell_i^1$ to the convolution of the NRL-modulated stimulus sequence $(\sum_m A_{mi} \mathbf{X}_m)$ with the HRF.

Note that the parameters β_1 and β_2 have been set to fixed values ($\beta_1 = \beta_2 = 0.8$ for the two approaches) and will not be estimated, as well as Γ and ℓ set as in [1].

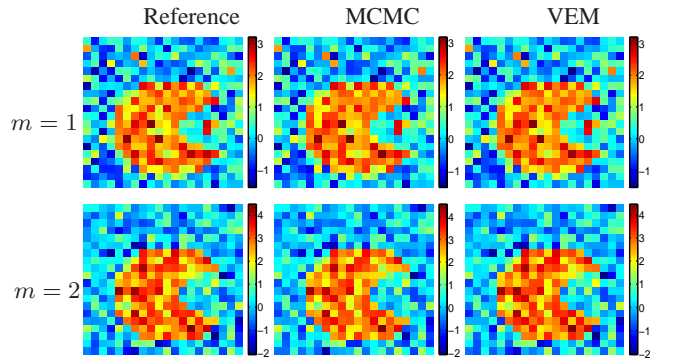


Fig. 1. Reference (left) and estimated NRLs amplitude using MCMC simulations (middle) and the proposed approach (right).

¹ \mathbf{P} was defined from a cosine transform basis and parameters ℓ_j were drawn from a normal distribution.

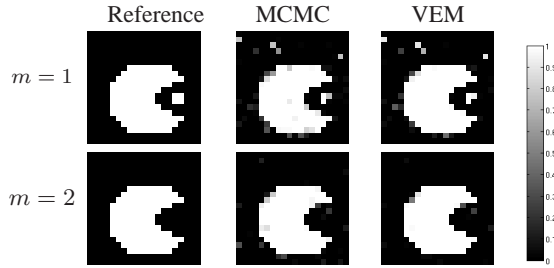


Fig. 2. Reference (left) and estimated labels (PPM) using MCMC simulations (middle) and the proposed approach (right).

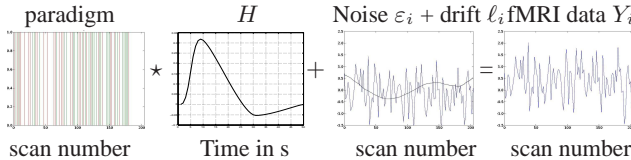


Fig. 3. Simulation of artificial fMRI datasets.

4.2. Performance comparison

We compare here our method based on VEM to the one in previous work [2] using intensive MCMC simulations. It can be observed from Fig. 2 that the two methods provide very close results in terms of estimated posterior activation probability maps (PPM), except for the first experimental condition $m = 1$. Estimated NRLs are also very similar both for $m = 1$ and $m = 2$ from a qualitative viewpoint (see Fig. 1). In order to compare the two approaches from a quantitative viewpoint, three different experiments have been conducted by varying the input Signal-to-Noise Ratio (SNR) of the simulated fMRI data. Table 1 shows SNR values of the simulated fMRI signal and the estimated NRLs w.r.t. the reference ones for the two considered conditions. It can be first noticed that since $\mu_{2,2} > \mu_{1,2}$, a higher SNR is always obtained for the NRLs corresponding to the second experimental condition ($m = 2$). As expected, reported SNR values indicate that the estimation precision increases with the input SNR. When comparing the two approaches, it seems that the proposed one is more robust to the noise in fMRI data. Note that displayed results in Figs. 1,2 and 4 correspond to Experiment 1.

Table 1. SNR (dB) values for the simulated fMRI signal Y and estimated NRLs.

	Y	MCMC		VEM	
		$m = 1$	$m = 2$	$m = 1$	$m = 2$
Exp. 1	11.86	44.81	45.27	50.96	55.13
Exp. 2	12.56	44.66	53.14	50.42	56.93
Exp. 3	15.91	47.97	53.82	52.59	58.41

As regards estimated HRFs, Fig. 4 shows that two approaches perform similarly in terms of estimation precision, mainly the time and amplitude of the peak. In terms of computational time, the results hereabove have been reached after 1 min on an Intel Core 2 - 2.26 GHz, while the MCMC-based approach took 4 min on the same architecture and programming language (Python).

5. CONCLUSION

We proposed an alternative to intensive MCMC sampling in the joint detection-estimation framework. Our contribution relies on a variational EM algorithm. Illustrations showed that this approach achieved similar and even better results than the MCMC-based approach. Results shown here were at the region level, on artificial

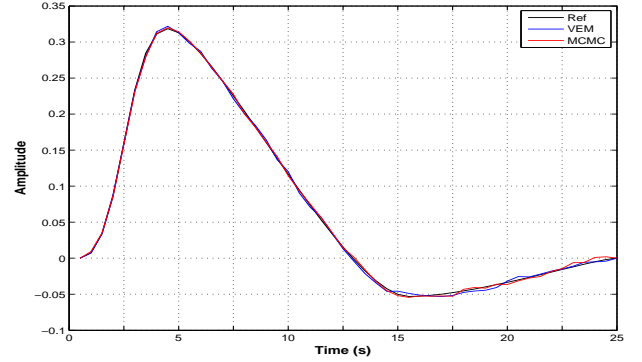


Fig. 4. Reference and estimated HRFs using the VEM and MCMC-based algorithms.

2D datasets of moderate size (20×20). Future work includes the application of our method to real 3D datasets on the whole brain (typically of size $96 \times 96 \times 40$). The differences between our method and the MCMC approach should then be even more significant both in terms of computational cost and results quality.

6. REFERENCES

- [1] S. Makni, J. Idier, T. Vincent, B. Thirion, G. Dehaene-Lambertz, and P. Ciuciu, "A fully Bayesian approach to the parcel-based detection-estimation of brain activity in fMRI," *Neuroimage*, vol. 41, no. 3, pp. 941–969, Jul. 2008.
- [2] T. Vincent, L. Risser, and P. Ciuciu, "Spatially adaptive mixture modeling for analysis of within-subject fMRI time series," *IEEE Trans. on Med. Imag.*, vol. 29, no. 4, pp. 1059–1074, Apr. 2010.
- [3] S. Ogawa, T. M. Lee, A. R. Kay, and D. W. Tank, "Brain magnetic resonance imaging with contrast dependent on blood oxygenation," *National Academy of Sciences*, vol. 87, pp. 9868–9872, Dec. 1990.
- [4] K. J. Friston, A. P. Holmes, J.-B. Poline, P. J. Grasby, S. C. R. Williams, R. S. J. Frackowiak, and R. Turner, "Analysis of fMRI time-series revisited," *Neuroimage*, vol. 2, pp. 45–53, 1995.
- [5] D. A. Handwerker, J. M. Ollinger, and M. D'Esposito, "Variation of BOLD hemodynamic responses across subjects and brain regions and their effects on statistical analyses," *Neuroimage*, vol. 21, no. 4, pp. 1639–1651, Apr. 2004.
- [6] J. Kershaw, B. A. Ardekani, and I. Kanno, "Application of bayesian inference to fMRI data analysis," *IEEE Trans. Med. Imaging.*, vol. 18, no. 12, pp. 1138–1153, Dec. 1999.
- [7] G. Marrelec, H. Benali, Ph. Ciuciu, M. Pelegrini-Issac, and J.-B. Poline, "Robust Bayesian estimation of the hemodynamic response function in event-related BOLD MRI using basic physiological information," *Human Brain Mapping*, vol. 19, no. 1, pp. 1–17, May 2003.
- [8] P. Ciuciu, J.B. Poline, G. Marrelec, J. Idier, Ch. Pallier, and H. Benali, "Unsupervised robust non-parametric estimation of the hemodynamic response function for any fMRI experiment," *IEEE Transactions on Medical Imaging*, vol. 22, no. 10, pp. 1235–1251, Oct 2003.
- [9] A.P. Dempster, A.P. Laird, and D.B. Rubin, "Maximum likelihood from incomplete data via the EM algorithm (with discussion)," *Journal of the Royal Statistical Society, Series B*, vol. 39, pp. 1–38, 1977.
- [10] R.M. Neal and G.E. Hinton, "A view of the EM algorithm that justifies incremental, sparse and other variants," in *Learning in Graphical Models*, Jordan, Ed., pp. 355–368. 1998.
- [11] M. Beal and Z. Ghahramani, "The variational Bayesian EM algorithm for incomplete data: with application to scoring graphical model structures," *Bayesian Statistics 7, University of Oxford Press*, pp. 453–464, 2002.
- [12] G. Celeux, F. Forbes, and N. Peyrard, "EM procedures using mean field-like approximations for Markov model-based image segmentation," *Pattern Recognition*, vol. 36, no. 1, pp. 131–144, 2003.